Science Advances

AAAS

advances.sciencemag.org/cgi/content/full/3/12/eaao3659/DC1

Supplementary Materials for

Chemical potential–electric double layer coupling in conjugated polymer–polyelectrolyte blends

Klas Tybrandt, Igor V. Zozoulenko, Magnus Berggren

Published 15 December 2017, *Sci. Adv.* **3**, eaao3659 (2017)
DOI: 10.1126/sciadv.aao3659

This PDF file includes:

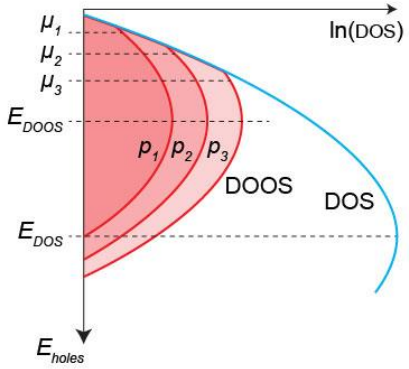

fig. S1. Chemical potential approximation. For a Gaussian DOS with low carrier concentration the density of occupied states (DOOS) can be approximated by another Gaussian centered around E_{DOOS}. The chemical potentials $\mu_1 < \mu_2 < \mu_3$ for the hole concentrations $p_1 < p_2 < p_3$ can therefore be approximated by eqn. (1).

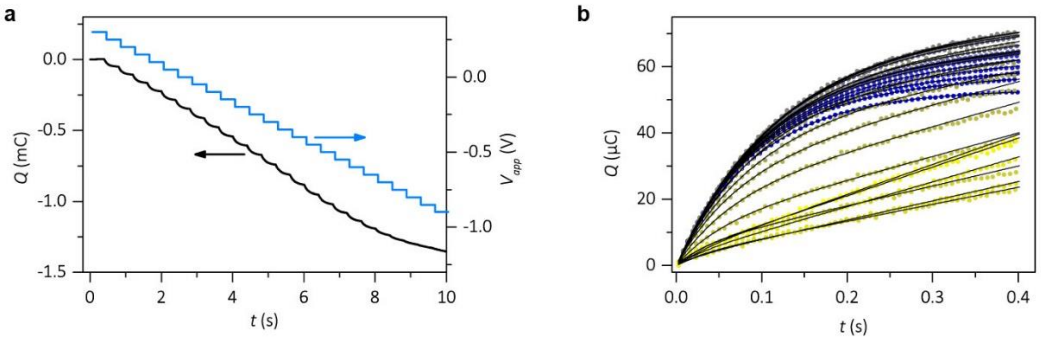

fig. S2. Charge measurements. (**a**) The charge carrier concentration within the PEDOT:PSS film is extracted by measuring the change in charge for -50 mV potential steps. (**b**) The charge for each step was estimated by fitting the function $Q(t) = Q_{EDL}(1\text{-}exp(-t/t_0))+I_f \cdot t$, where Q_{EDL} constitutes the charge in the PEDOT:PSS while I_f is the faradaic current arising from side reactions. The fit was performed in the interval 0-0.3 s where $I_f \cdot t$ was linear. The charge vs V_{app} was calculated by $Q(V_{app}) = \Sigma Q[-0.875, V_{app}]$ with $Q(-0.875)$ set as the zero reference level as it was the minimum for $Q(V)$.

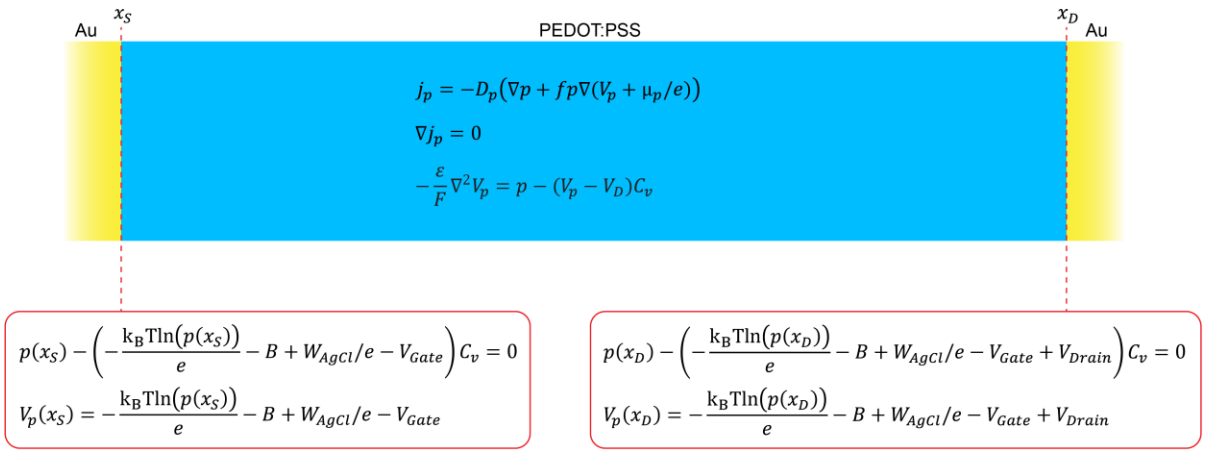

fig. S3. OECT equations. The PEDOT phase is modelled by the drift-diffusion equations and Poison's equation, which couples the charging of the PEDOT phase to the PSS phase by the EDL. For steady state, the potential in the PSS phase (V_C) can be approximated by the Donnan potential V_D. The boundary conditions at the metal contact are derived from equating the electrochemical potentials on the two sides of the boundary and assuming zero space charge at the interface.

table S1. Simulation parameter values.

General	
T	300 K
PEDOT phase	
B	-0.767 V
D_p	2.05e-5*(1.05-1.08/(1+exp((p-71.0)/22.8))) m^2/s
C_V	204 mol/(m^3V)
PSS phase	
V_D	-0.0717 V
c_{fix}	2400 mol/m^3
D_{c+}	3.34e-10 m^2/s
D_{c-}	5.08e-10 m^2/s
Electrolyte phase	
D_{c+}	13.3e-10 m^2/s
D_{c-}	20.3e-10 m^2/s
c_0	150 mol/m^3
OECT	
w, l, h	40, 20, 0.05 µm
CV	
Scan rate	200 mV/s
x_P	600 nm
x_{Elec}	7.91 mm
Pulse	
x_P	281 nm
x_{Elec}	7.91 mm
EIS	
x_P	154 nm
x_{Elec}	4.02 mm
Moving front	
x_P	10 mm
x_{Elec}	60 µm

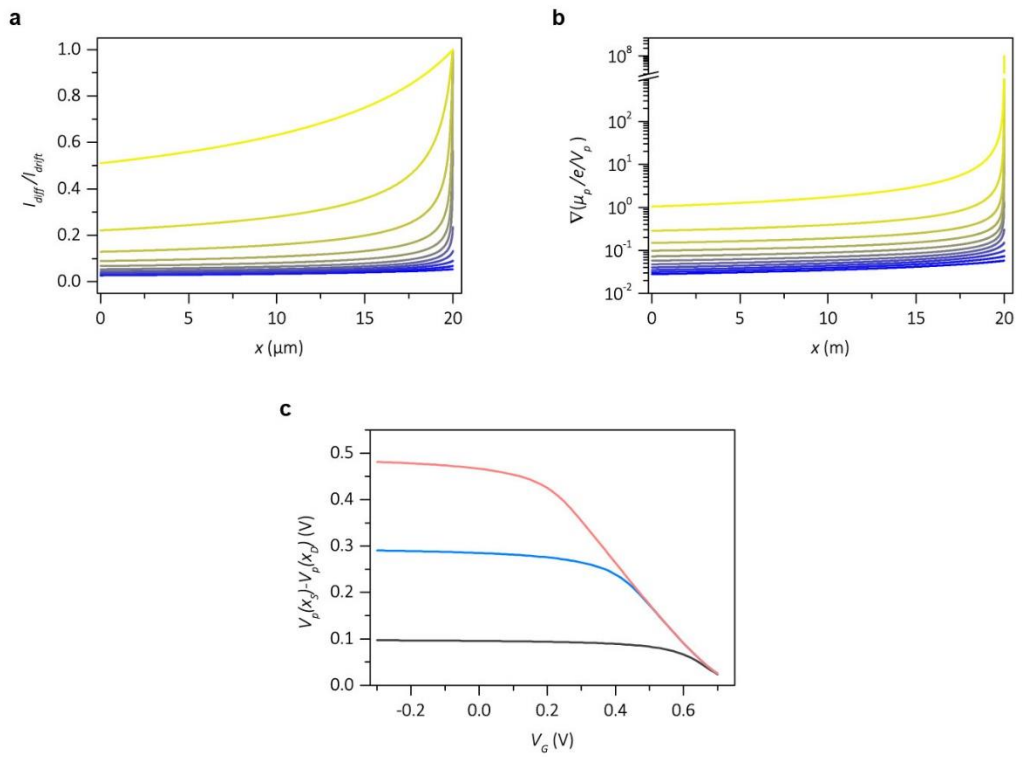

fig. S4. Transport in OECTs. (**a**) The ratio of diffusion to drift transport for V_G = -0.3 V (blue) to 0.7 V (yellow). The diffusion contribution is small for high carrier concentrations but becomes important for lower concentrations. (**b**) The ratio of the contribution from the chemical potential correction to the regular drift term for V_G = -0.3 V (blue) to 0.7 V (yellow). The correction becomes substantial for lower carrier concentrations. (**c**) The difference in electrostatic potential between the source and drain sides of the channel decreases for higher gate potentials (red V_D = -0.5 V, blue V_D = -0.3 V, grey V_D = -0.1 V). However, this is compensated by the chemical potential correction so that the effective potential difference remains the same for all V_G (Fig. 2e).

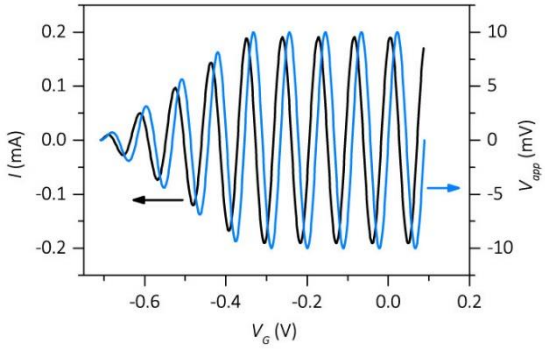

fig. S5. Example of the simulation of EIS data. To shorten the stabilization time, the applied oscillating potential (10 mV, 11.29 Hz) is gradually ramped up. The current is calculated from the change in the amount of charge carriers within the film over time. The difference in phase between the voltage and the current originates from the capacitive nature of the system.

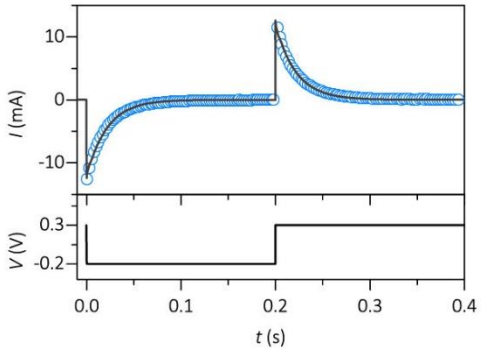

fig. S6. Square-wave response. The calculated current (○) fits the experimental data (line) well for an applied square wave (-0.2 V to 0.3 V).

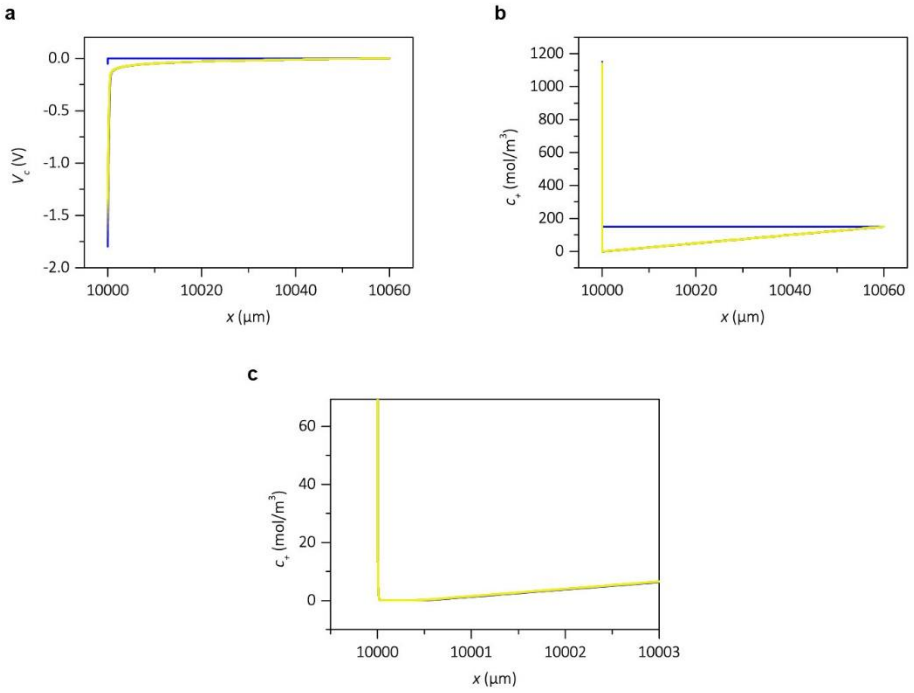

fig. S7. Concentration polarization at the electrolyte interface in moving front simulation [0 s (blue line) to 45 s (yellow line)]. (**a**) Most of the potential is dropped next to the PEDOT:PSS-electrolyte at x = 10 mm. (**b**) This is due to a common phenomenon called concentration polarization, as the concentration becomes close to zero at the cation selective interface. (**c**) The depleted region extends approximately 500 nm out from the PEDOT:PSS.

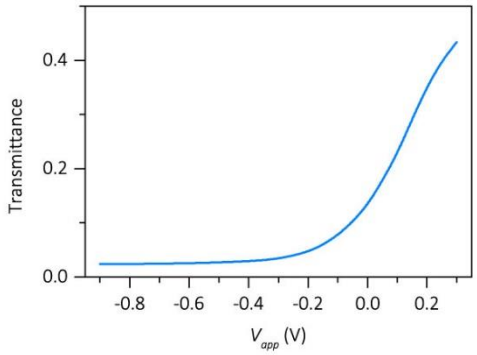

fig. S8. PEDOT:PSS transmittance at the 600-nm peak for varied potentials [adopted from Sonmez *et al*. (*33*)].

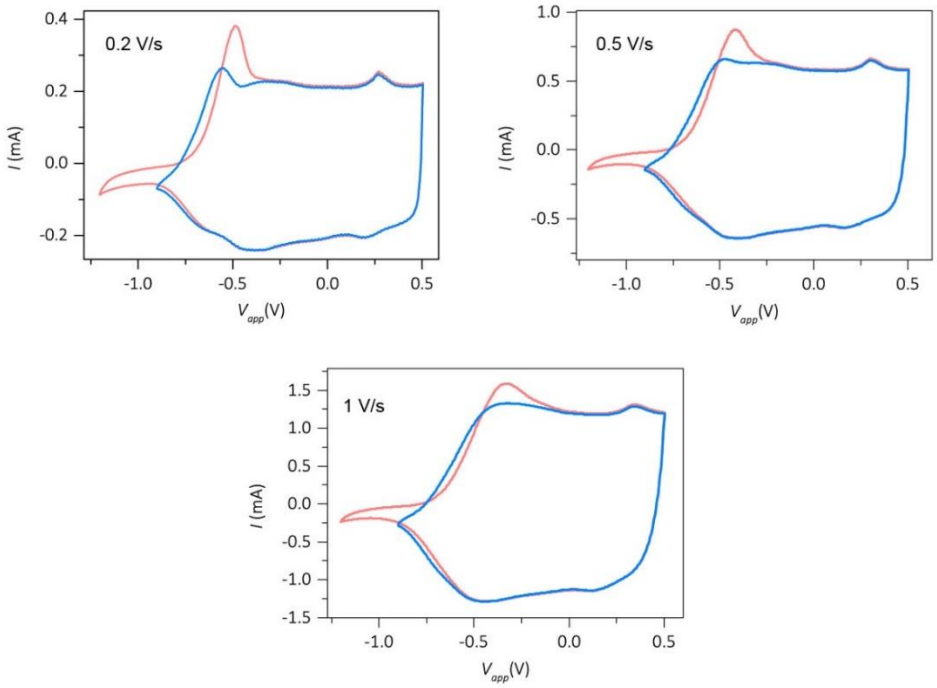

fig. S9. CVs of 600-nm-thick PEDOT:PSS films. The shown traces are from repeated scans in order for them to stabilize, with the [-0.9, 0.5] V scan performed first. The shape of the CV for V_{app} < 0 V depends on the lower boundary of the scan, with a peak appearing in the forward scan at approximately -0.4 V when the lower boundary is -1.2 V. The fact that the traces are identical for higher potentials but starts to deviate at -0.5 V in the backward scan direction indicates that a permanent change in the conductivity has been induced by the negative potential.

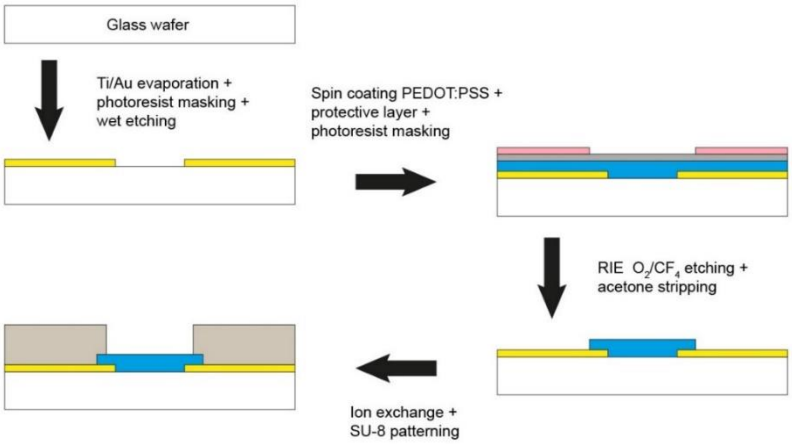

fig. S10. OECT fabrication scheme. The OECTs are fabricated on glass wafers with regular microfabrication techniques. The critical step is to protect the OECT channel from contact with the photoresist and developer to avoid effecting the performance of the channel material.